Tellus (1995), 47B, 122–144
Printed in Belgium – all rights reserved

TELLUS
ISSN 0280–6509

Modelling the seasonal course of the upper ocean pCO_2 (II). Validation of the model and sensitivity studies

By DAVID ANTOINE* and ANDRÉ MOREL, *Laboratoire de Physique et Chimie Marines, Univ. P. & M. Curie, CNRS (URA 353), 06230, Villefranche sur Mer, France*

(Manuscript received 12 November 1993; in final form 1 August 1994)

ABSTRACT

A one-dimensional model was developed, aiming at the simulation of the seasonal course of the upper-ocean pCO_2. This model is validated here, by comparing its outputs with field data, at the Ocean Weathership Station Papa in the Northeast Pacific Ocean (from 1975 to 1977). This simulation emphazises the leading role of biology in changing the inorganic carbon content at this station, compared to those of eddy diffusivity, entrainment and air-sea exchange. Complex and intricated dependences of pCO_2 variations on temperature, ΣCO_2 and TA are analysed. On the occasion of a comparison of the model with that of Taylor et al., the pitfalls of univocal correlations between the sea-surface pCO_2, temperature and Chl at a given site are put in evidence on the basis of their complex and divergent annual evolutions. Sensitivity tests quantitatively show the importance for the model of (i) the representation of the chlorophyll cycle, (ii) the mean value selected for the *f*-ratio. Some possible developments of the model, and its applications in view of assimilating remotely-sensed data are discussed.

1. Introduction

With the purpose of simulating the annual course of the upper-ocean pCO_2, a one-dimensional model was developed; it is particularly designed to quantify the relative role of physical and biological processes in the modulation of the pCO_2 (Antoine and Morel, this issue). Briefly, this model accounts for (i) the variations in the physical environment, i.e., in the mixed-layer depth, temperature and eddy diffusivity, in response to the external forcing, (ii) the photosynthetic carbon fixation, (iii) the fate of the organic carbon produced through photosynthesis, either locally recycled or exported down to deep waters, and parameterised by using the temporal variations of the chlorophyll content combined with a *f*-ratio, (iv) the chemistry of CO_2 in seawater, allowing the pCO_2 inside the mixed layer to be computed from the total inorganic carbon (ΣCO_2) and total alkalinity (TA) contents. The carbon fluxes resulting from air-sea exchange, upward transport, and net primary production are thus simultaneously assessed. The model is deliberately developed under the proviso of making use of remotely-sensed information about chlorophyll, wind, temperature and irradiance; nevertheless a minimal a priori knowledge of the oceanic zone under consideration is needed. Even if a light-photosynthesis model is incrusted in the general model, the algal biomass evolution is not predicted. On the contrary, the carbon-based biological compartment is driven by the chlorophyll concentration evolution, as detectable from space.

A validation of the model at the Ocean Weathership Station PAPA (OWSP) in the Gulf of Alaska is presented here, and the relative roles of the various processes governing the CO_2 evolution are assessed. The possible existence of correlations between SST and pCO_2, and between sea-surface chlorophyll concentration and pCO_2 is then examined within the frame of a comparison of a simplified version of the present model with

* Corresponding author.

another modelling investigation (Taylor et al., 1991). Finally, the needed developments or simplifications of the model in view of assimilating future satellite information at large scale are discussed.

2. Validation of the model at the Ocean Weathership Station Papa (OWSP)

Over a period of 30 years (1949–1981), a considerable database was set up by the Canadian Environmental Service, from the meteorological and oceanographic parameters recorded at Ocean Weathership Station Papa, located in the Gulf of Alaska (50°N, 145°W). Along with the usual measurements (SST, salinity, wind speed...), oceanic and atmospheric pCO_2 were monitored from 1973 to 1978. These measurements were recently published and analysed by Wong and Chan (1991). Sea-surface pCO_2 was more regularly recorded during 1975, 1976 and 1977, and oxygen and nitrate concentrations were also determined. These three years are therefore selected for a validation of the present modelling.

OWSP is located at the transition zone between the North Pacific drift and the Alaska gyre system, what allows the horizontal advection to be considered as negligible (Gaspar et al., 1990). This feature results in favourable conditions when validating a one-dimensional model. Furthermore, sea-surface salinity is rather constant throughout the year (around 32.8 psu), and the water budget (evaporation versus precipitation) being approximately balanced, it does not play an important role in the physical forcing at OWSP (Martin, 1985). Mixed-layer depth exhibits a notable seasonality, and extends in January–February down to a permanent halocline, at about 110 m. After several short-term retrait events in March–April, a steady stratification occurs in summer resulting in a thin mixed layer (about 20 m). The erosion of the seasonal thermocline begins in early fall, and progressively leads to the winter convective system. The autumn cooling is mostly due to episodic stormy events (Large et al., 1986). Eddy diffusivities around 10^{-5} m^2 s^{-1} were estimated at the base of the mixed layer in summer, while values greater than 10^{-4} m^2 s^{-1} could occur in winter (Emerson et al., 1991; Large et al., 1986).

OWSP is a representative example of the situation generally prevailing in the Subarctic Pacific ocean, with relatively low and weakly variable Chl concentrations of about 0.45 mg(Chl) m^{-3}. Reduced blooms (1 to 2 mg(Chl) m^{-3}) appear episodically, usually from May to September (Miller et al., 1991). This algal biomass steadiness is also confirmed by ocean-colour imagery (Yoder et al., 1993). Surface waters, however, are never nutrient-depleted, with concentrations varying between 5 and 15 mmol NO_3 m^{-3} (Frost, 1991). These two somewhat contradictory observations could originate from intense grazing pressure (Booth et al., 1988), or from ammonium-limitation of nitrate uptake (Wheeler and Kokkinakis, 1990). Such features are typical of a high-nutrient, low-chlorophyll, zone (HNLC) (Miller et al., 1991).

Primary production exhibits a marked seasonality, resulting mainly from physical environment (irradiation and temperature variations), with a maximum in summer (Frost, 1991), when approximately 70% of the annual production seems to occur (Emerson et al., 1991). Sea-surface pCO_2 evolution was described in Wong and Chan (1991). Even if OWSP is on average a sink for CO_2, with a mean annual entering flux of about 0.7 mol CO_2 m^{-2} year^{-1}, evasion of CO_2 could have occurred in summer 1975. An outgassing O_2 flux, of about 30 mmol O_2 m^{-2} d^{-1}, was estimated by Emerson et al. (1991), for the years 1987 and 1988.

The model is operated as follows (see Table 1 for symbols and units).

2.1. *Computation of the surface heat fluxes*

Heat fluxes are computed from the three-hourly records of (i) SST, (ii) air temperature, (iii) wind speed at 10 m height, (iv) sea-level barometric pressure and (v) total cloudiness index. Some missing data (about 5% of the total) were interpolated between the surrounding measurements. The computed surface heat fluxes (Table 2, and Fig. 1a) are in close agreement with those computed for another period (1969–1972) by Tricot (1985), and adopted by Gaspar et al. (1990). The heat budget cumulated over the three years exhibits a final excess of 3.1 W m^{-2} (Table 2). This gain should correspond to an increase of about 0.2°C within the upper 110-m layer, actually comparable with the increase as derived from bathythermographic records (about 0.3°C). This agreement is somewhat fortuitous, as the accuracy of the heat fluxes estimates cannot be better than

Table 1. *Symbols and units used in the text*

pCO_2	oceanic CO_2 partial pressure (μatm)
ΣCO_2	total inorganic carbon concentration in seawater (μmol kg^{-1})
ΔpCO_2	CO_2 partial pressure difference at the air-sea interface (μatm)
TA	total alkalinity in the mixed layer (μequ kg^{-1})
NO_3	nitrate concentration (mol m^{-3})
O_2	oxygen concentration (mol m^{-3})
Chl	chlorophyll concentration (mg Chl m^{-3})
Z_{ml}	depth of the mixed layer (m)
EKE	eddy kinetic energy (m^2 s^{-2})
K_z	eddy diffusivity coefficient (m^2 s^{-1}, and subscript ml for its value at the base of the mixed layer)
SST	sea-surface temperature (°C)
P	net primary production (gC m^{-2} d^{-1})
R	local recycling of the organic carbon produced through photosynthesis (gC m^{-2} d^{-1})
C-to-Chl	carbon-to-chlorophyll ratio (g/g)
f	ratio of new-to-total production

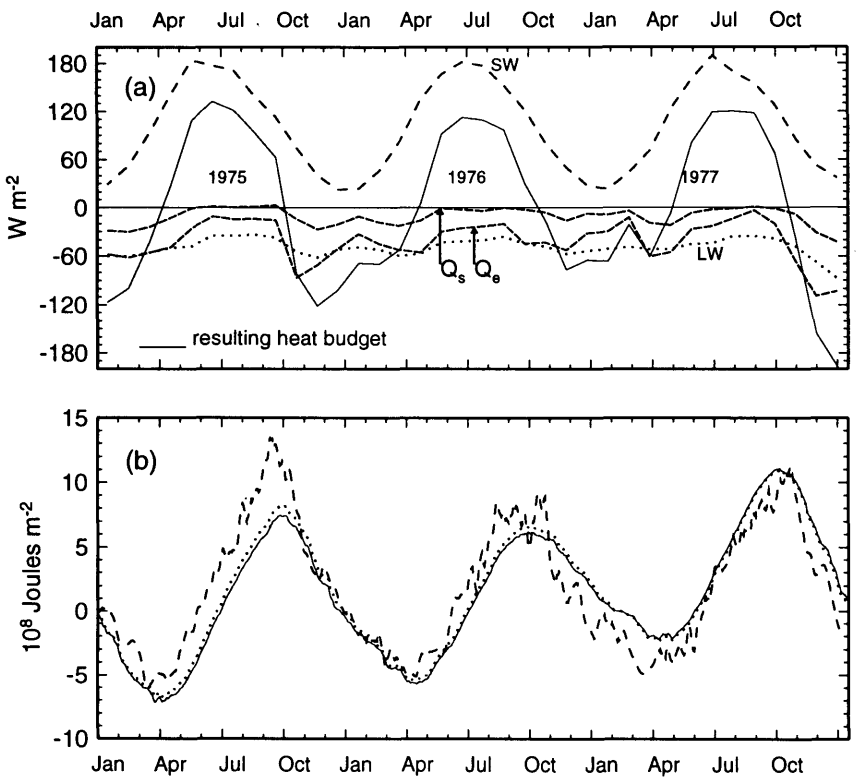

Fig. 1. (a) Annual courses of the various heat fluxes, computed from the three-hourly meteorological records at OWSP, and shown as monthly means for the sake of clarity. The solid line is the heat budget resulting from the sum of the sensible heat flux, Q_s, the total radiation impinging at sea level, SW, the latent heat flux, Q_e, and the net long-wave radiations budget, LW. The sign of the heat budget is reversed in March–April and October. (b) temporal variations of the heat content within the upper (110 m) layer. The solid curve is the integration of the surface heat budget shown in a; the dashed curve was obtained by using the bathythermographic records from 0 down to 110 m; the dotted curve is obtained by integrating the temperature profiles produced by the EKE model.

Table 2. *Upper part: mean values of the observed wind speed and sea-surface temperature at OWSP*

		1975	1976	1977	mean	1969–1972
observed	wind speed ($m\ s^{-1}$)	9.3	9.3	9.6	—	—
	sea-surface temperature (°C)	7.67	7.77	8.04	—	—
computed ($W\ m^{-2}$)	solar flux (SW)	101.8	102.3	101.1	101.7	101
	net long-wave budget (LW)	−48.8	−48.9	−48.1	−48.6	−40
	sensible heat flux (Q_s)	−12.8	−9	−11.8	−11.2	−57
	latent heat flux (Q_e)	−43.2	−38.1	−41.8	−41 (−52.2)	
	heat budget ($SW + LW + Q_s + Q_e$)	−2.8	6.5	−0.6	3.1	4

Lower part: mean values of sea-surface heat fluxes as computed from the three-hourly meteorological records. A slight increase in temperature is observed between 1975 and 1977, in correspondance with the weak heat gain computed over the 3 years. The last column provides mean values for the period covering the years 1969 to 1972, taken in Gaspar (1988).

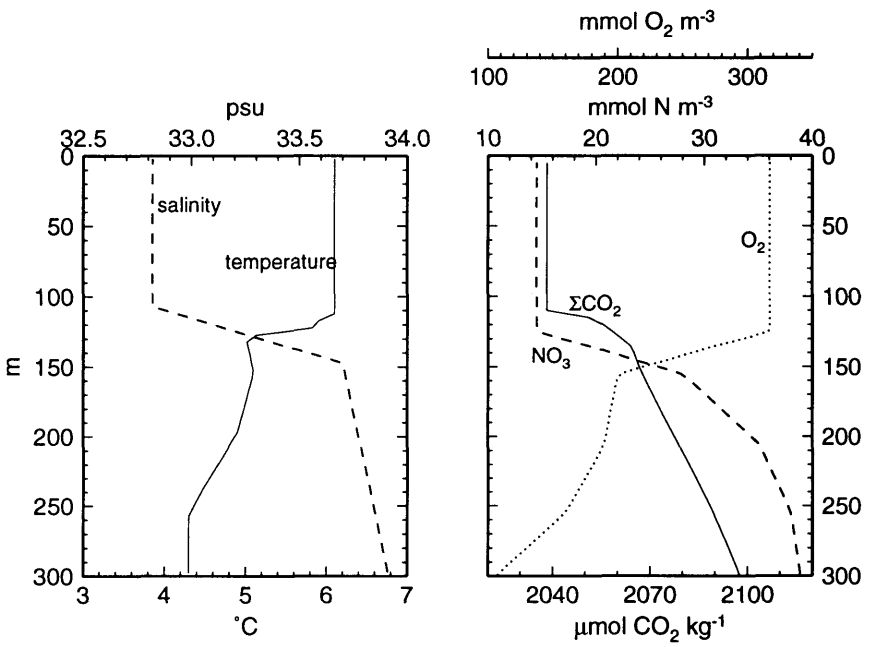

Fig. 2. Vertical profiles used as initial conditions (1 January 1975) of temperature (from bathythermographic records), salinity (climatological profile), nitrate and oxygen (from measurements), and ΣCO_2.

3 W m^{-2}. The variations of the heat content of the upper (110 m) layer, either deduced from the surface heat fluxes, or derived from the bathythermographic records, or finally computed from the temperatures obtained via the EKE model, are very close (Fig. 1b). This general agreement confirms that the surface heat fluxes parameterisation is able to reproduce the upper-ocean temperature variations at OWSP in a rather accurate way.

2.2. *Physical characteristics of the water column obtained via the EKE*

A climatological salinity profile, taken from Levitus (1982), and a bathythermograph profile (Fig. 2) are used when initialising the EKE model, on the 1st of January, 1975. The minimum threshold value for the turbulent kinetic energy is set at 10^{-6} m^2 s^{-2}.

The annual courses of the mixed-layer temperature at OWSP are very well reproduced by the EKE model (Fig. 3a). The agreement between measured and computed temperatures is excellent, without any bias. The mean difference is totally negligible ($+0.014$°C), and the standard deviation is 0.39°C. When the solar heating of the upper layers is computed without taking into account the actual Chl concentration, but rather by using the same Jerlov's optical water type (type II) throughout the year, the mean difference and standard deviation turns out to be -0.12 and 0.45°C, respectively. The interannual differences in the temperature attained in summer are very well reproduced, whereas a slight drift appears in winter. It can be argued that a kind of restoring is implicitely included in the present computation, as the SST "meteorological" data are used to compute the heat flux terms. The model has been operated in an entirely free mode, by using the temperature computed each three hours for the upper layer (5 m thick, in EKE) to compute the heat exchange for the following 3 h period. This trial has not revealed any perceptible deviation, even after three years, with respect to the results obtained by using the measured SST.

The mixed-layer depth evolution (Fig. 3b) is consistent with the result of other modelling studies (Garçon et al., 1992), as well as with field data (Martin, 1985; Gaspar, 1988). A certain interannual variability is observed for the onset of the stratification. Finally, the eddy diffusivity just below the mixed layer (Fig. 3c), exhibits values, from less than 10^{-3} m^2 s^{-1} (about $6 \cdot 10^{-4}$) to 10^{-5} m^2 s^{-1}, comparable to other estimates (Emerson et al., 1991; Large et al., 1986). The lower values are obviously attained when mixing is minimal in summer, but also in winter, when the mixed layer extends down to the permanent halocline. In conclusion, the physical characteristics of the water column, as modelled via the EKE model, very close to the observed conditions, are believed to be realistic.

2.3. *Chlorophyll concentrations and net primary production*

The Chl concentrations measured at OWSP in 1975 and 1976 show frequent and extended gaps with a mean value of 0.45 mg(Chl) m^{-3}. Episodic higher concentrations appeared in June and July 1975, but not in 1976. From this irregular time-serie for sea-surface Chl, three types of Chl "cycles" are thereafter considered. The first one is a linear interpolation between measurements, and covers the period from 1975 to 1976. The second one is simply a constant concentration equal to the mean value. The third one consists of a hypothetical and unique annual cycle, reproduced over the three years, and built as a Gaussian curve superimposed on the constant concentration of 0.45 mg(Chl) m^{-3} (see Fig. 4a). The choice of the position of the summer maximum (day number 225), with a peak value of 1.6 mg(Chl) m^{-3}, is supported by the relative depletion of NO_3 observed during the period of mixed-layer stability. This choice and the peak value seem also reasonable when considering long-time series of Chl determinations at OWSP (see also Fig. 4a). Note that Garçon et al. (1992) also adopted a Gaussian curve for the annual course of primary production, as being the most suitable when reproducing the O_2 data. The vertical profiles for Chl were inferred from the sea-surface concentration alone (Fig. 5), by using the two sets of equations of Morel and Berthon (1989), for stratified and not stratified situations, respectively.

The net primary production, P, (gC m^{-2} d^{-1}) is computed with the three kinds of chlorophyll cycles (Fig. 4c).

2.4. *Other initial conditions and prescribed parameters*

The f-ratio at OWSP, derived from ^{15}N measurements (Wheeler and Kokkinakis, 1990) does

not exhibit clear seasonal trends, except that f is apparently depressed during August (Fig. 4b). As a consequence, and also in absence of data in winter, a constant f-ratio of 0.36 (the mean of Wheeler's estimates) is assumed in a first step. The C-to-Chl ratio was measured in May 1988 by Frost (1991), and his value, 53 (g/g), is adopted and kept constant throughout the year.

The ΣCO_2 vertical profile used as initial condition (Fig. 2) was built from the measurements made at the surface in January 1975 by Wong and Chan (1991), namely 2040 μmol kg^{-1}, and from a

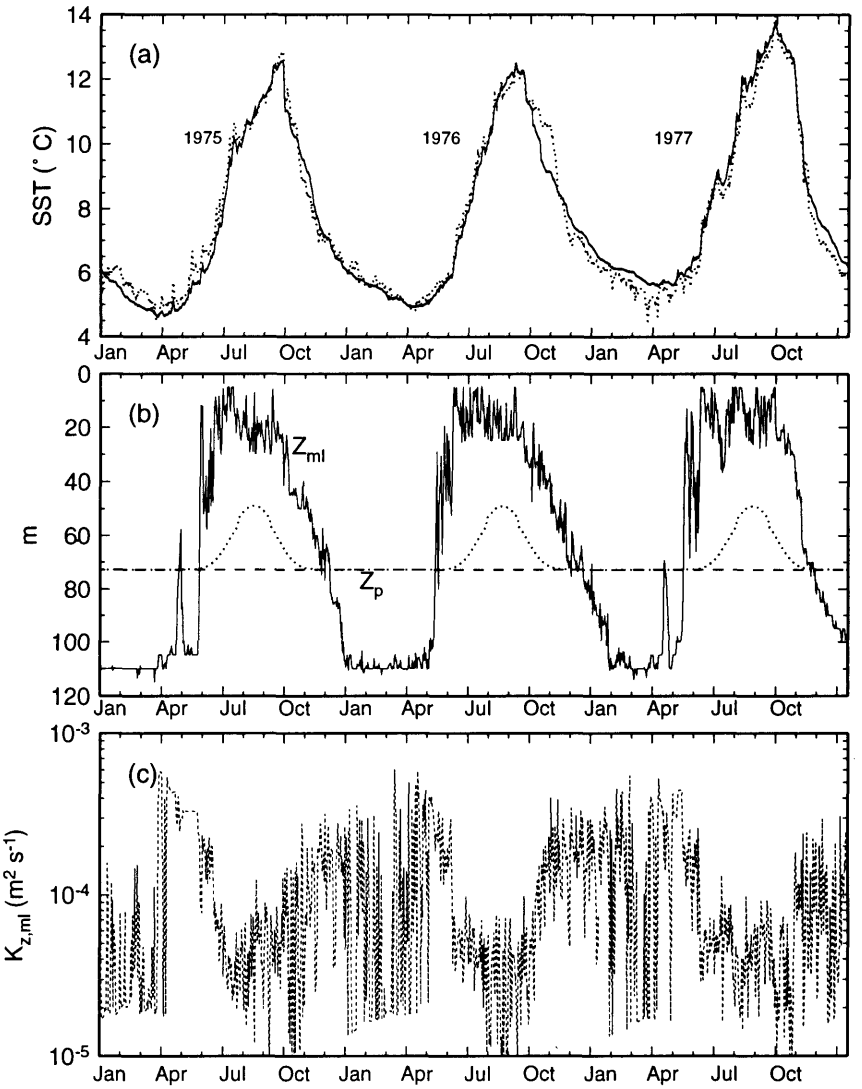

Fig. 3. Annual courses at OWSP of (a) SST: the heavy curve is the temperature from the EKE model and the light curve is from the three-hourly records (b) the mixed-layer depth from the EKE model (heating of the upper layers was computed with the Gaussian Chl cycle of Fig. 4), and the depth of the productive layer, as computed either from a constant Chl concentration (0.45 mg(Chl) m^{-3}, $Z_p = 72$ m), or from the Chl Gaussian cycle (c) the eddy diffusivities at the base of the mixed layer (log scale).

climatological value typical for the deep North Pacific, namely 2100 μmol kg^{-1} (Bacastow and Maier-Reimer, 1990). Salinity is kept constant (32.8 psu), and the biologically-induced variations in TA are not here taken into account. Therefore, a unique value for TA is necessary. TA is thus set at 2215 μequ kg^{-1}, as calculated at station Papa in January 1975 by Wong and Chan (1991), and kept constant throughout the three years. With the ΣCO_2 initial vertical profile, and those for O_2 and NO_3 (Fig. 2), the model is thereafter freely run over the three consecutive years without any introduction of external data or restoring to obtain a better fit with the observations. The three annual courses for atmospheric pCO_2 were computed by using the CO_2 mole fraction, taken in Chan and

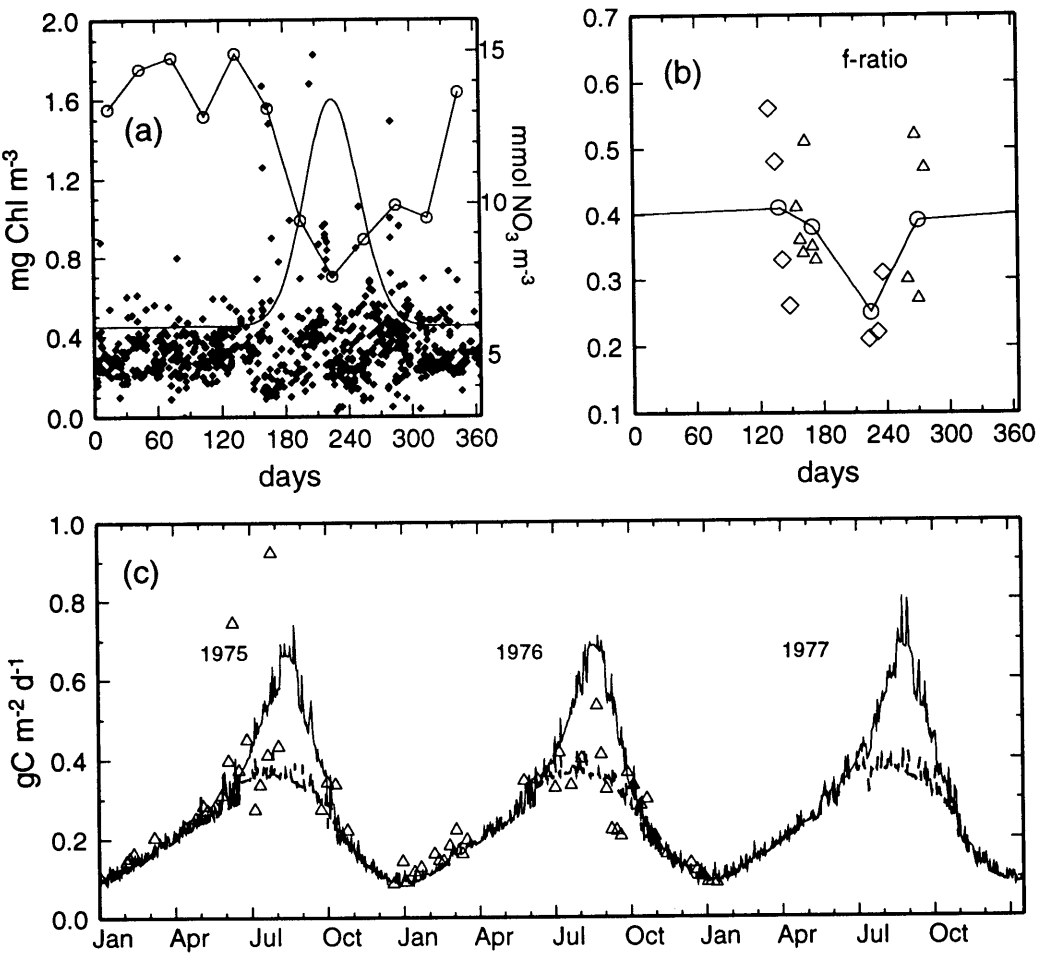

Fig. 4. (a) Compilation of 20 years (1958–1977) of sea-surface Chl determinations at station Papa (diamonds, left scale), and monthly means of the nitrate measurements made over the same years (circles linked by straight line, right scale). The hypothetical Chl Gaussian cycle is also shown. (b) Field data of the *f*-ratio at OWSP obtained, from ^{15}N experiments (Wheeler and Kokkinakis, 1990), in 1987 (triangles) and 1988 (diamonds). Monthly means of these field values (four) are displayed as circles and linked by straight line. (c) Discrete values of the net primary production, computed from the Chl concentrations measured in 1975 and 1976 (triangles), and the 3-year course of the net primary production, when computed with a constant Chl concentration (0.45 mg(Chl) m^{-3}, dashed line), or with the Gaussian cycle (solid line). The weak interannual differences in carbon fixation are due to variations in the light environment, as well as in temperature.

Wong (1990), the barometric pressure, and the saturated water vapor pressure at sea surface temperature. The oxygen partial pressure was kept constant (0.21 atmosphere).

2.5. *Results: annual courses of mixed-layer pCO_2, O_2 and NO_3*

In a first run of the model, the ocean was considered as an abiotic medium, even if the initial ΣCO_2 vertical profile actually results, at least partly, from the former biological activity. In such a simulation, where biological activity has suddenly ceased, it is assumed that the disrupted system will evolve towards a new equilibrium. The evolution (Fig. 6a) leaves to think that a newly balanced system is not yet reached after three years, as pCO_2 is persistently increasing. A 20-year repeated simulation, making use of the physical forcing of 1975 only, results in a steady pCO_2 cycle; the final values exceed by 20 to 50 μatm the initial ones (Fig. 6b). In this abiotic, physically stable system, the upward CO_2 flux originating from CO_2-rich deep waters is balanced owing to an equal outgassing. The net effect of the biological activity is clearly to maintain the pCO_2 level well below that of an abiotic ocean under the same physical constraints.

A constant Chl concentration of 0.45 mg(Chl) m^{-3} is used as input in a second run, to verify if this only introduction is able to bring back the pCO_2 values toward realistic levels. Indeed, the resulting cycle falls within the range of observed values, at least during winter and autumn (Fig. 7a). In summer, however, the simulated values exceed the actual ones, presumably because the CO_2 uptake by algae has been underestimated.

When the model is fed with the observed (and interpolated) Chl concentrations, the result (Fig. 7b, 1975 and 1976 only) is not greatly improved compared to that obtained with a con-

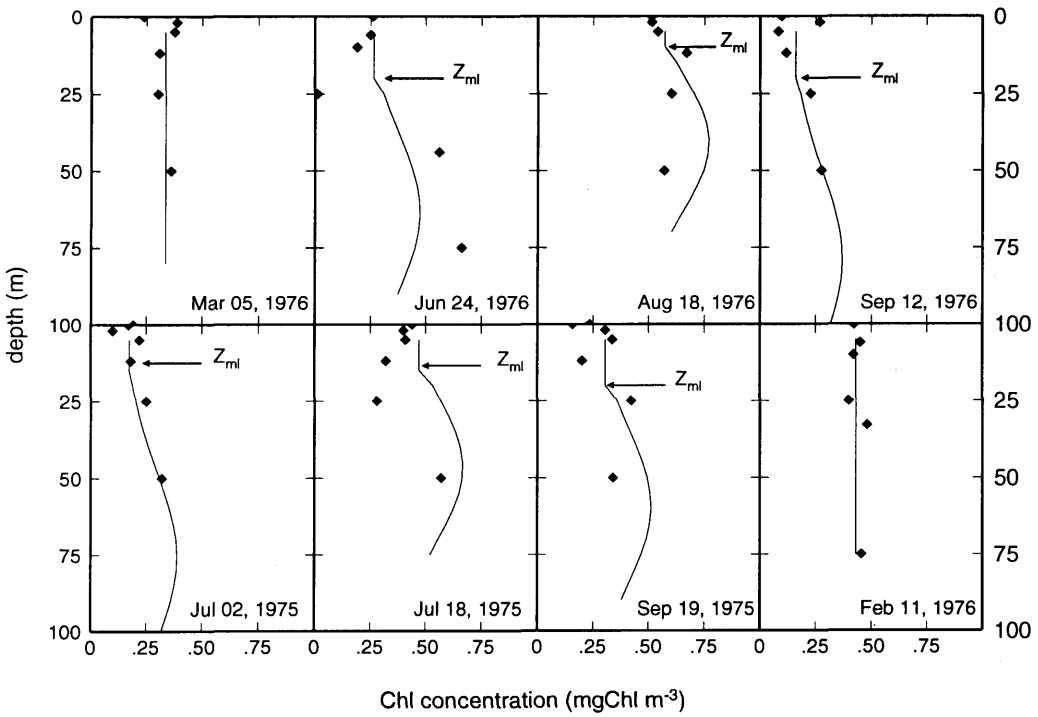

Fig. 5. Examples of vertical Chl profiles reconstructed from the concentration measured at the sea surface, compared to measured profiles (diamonds). The measured profiles (when they exist) were not used in the simulations, to remain consistent with the proviso that the model must be fed only with the Chl concentration at the sea surface, as detectable from space. Mixed layer depths are indicated when less than 100 m.

Tellus B/47/1/2-9

stant Chl concentration, probably because of the under-sampling of Chl. As suggested by the observation of large drawdowns of nitrate and pCO_2 in summer, the algal biomass might temporarily reach higher levels, missing in the data set. An accurate prediction of the pCO_2 would require that the Chl evolution be described with a temporal resolution similar to that used for the physics of the mixed layer. This is particularly true at Station Papa, because short-time variations in biology inside the thin mixed layer established in summer are quickly reacting on pCO_2, is spite of their weak amplitude.

The three-year pCO_2 course is finally computed by introducing the Chl Gaussian cycle. The agreement with the measured pCO_2 is much better (Fig. 7c), with a mean ratio of modeled-to-measured pCO_2 of 1 and a standard deviation of 7 μatm. In addition, the annual courses of nitrate and oxygen, which are by-products of the simulation, are also fairly well reproduced (Fig. 8). It can be reasonably concluded that the bulk seasonal variations in all parameters are well captured by the model, as well as many small-scale details.

2.6. *CO_2, O_2 and NO_3 annual fluxes derived from temporal evolutions*

The resulting annual fluxes in C, O_2 and NO_3 can be established (Table 3) and compared to some estimates derived from field experiments. On average, the computed photosynthetic carbon fixation amounts to 104 gC m^{-2} y^{-1}, equivalent to 0.285 gC m^{-2} d^{-1} on a daily basis. When considering only the May-to-August period, the mean value amounts to 0.50 gC m^{-2} d^{-1}, within the range of those measured for the same period (0.24 to 1.3, mean value 0.6 gC m^{-2} d^{-1}), but in 1984, by Miller et al. (1991). Old data (now

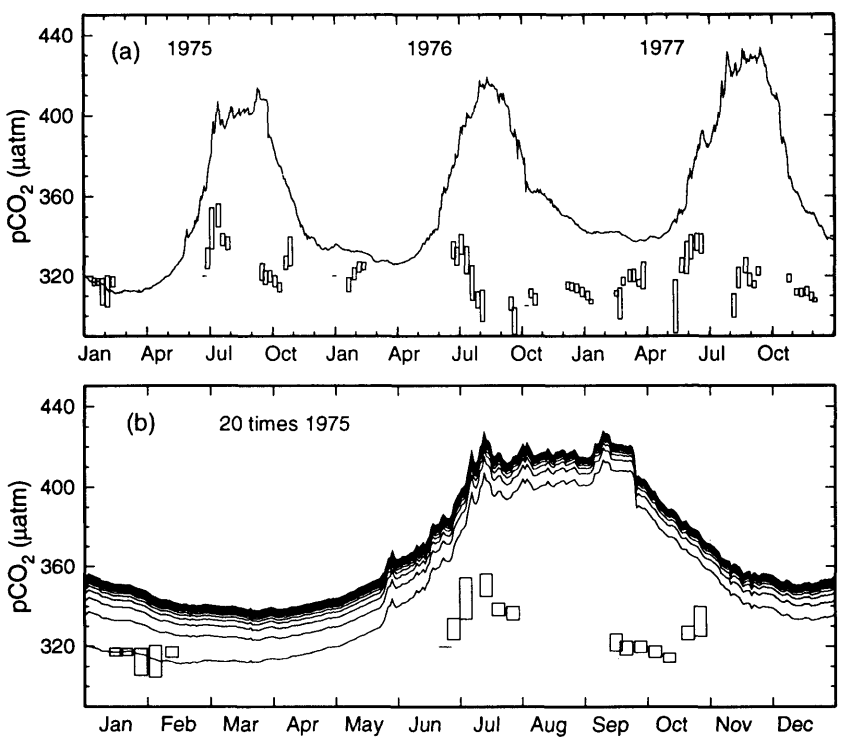

Fig. 6. (a) Annual courses at OWSP of the mixed-layer pCO_2 computed for an abiotic ocean; the rectangular boxes represent measured pCO_2 values averaged over one week, and their heights represent one standard deviation (see Table 2 in Wong and Chan (1991)). (b) mixed-layer pCO_2 cycles obtained by running the abiotic model for twenty years and repeatedly imposing the physical constraints of 1975; boxes are as in (a).

questionable) were lower by a factor of 2 (McAllister et al., 1960). A slight interannual variability appears in the computed annual primary productions ($\pm 3\%$ around the mean, see Table 3), even if they are estimated from the same Gaussian cycle for sea-surface Chl. This is mainly due to the change in temperature and irradiance.

The new production is steadily around 37 gC $m^{-2} y^{-1}$ (or 101 mgC $m^{-2} d^{-1}$), as a straightforward consequence of the choice of the f-ratio. New production was inferred from oxygen mass balance calculations, resulting in a value of 140 mgC $m^{-2} d^{-1}$ for summers 1987 and 1988 (Emerson et al., 1991), or more generally in values in the range 100–300 mgC $m^{-2} d^{-1}$ for the entire 10 year period, from 1969 to 1978 (Emerson, 1987). The relative agreement in terms of new production obviously extends to the correlative

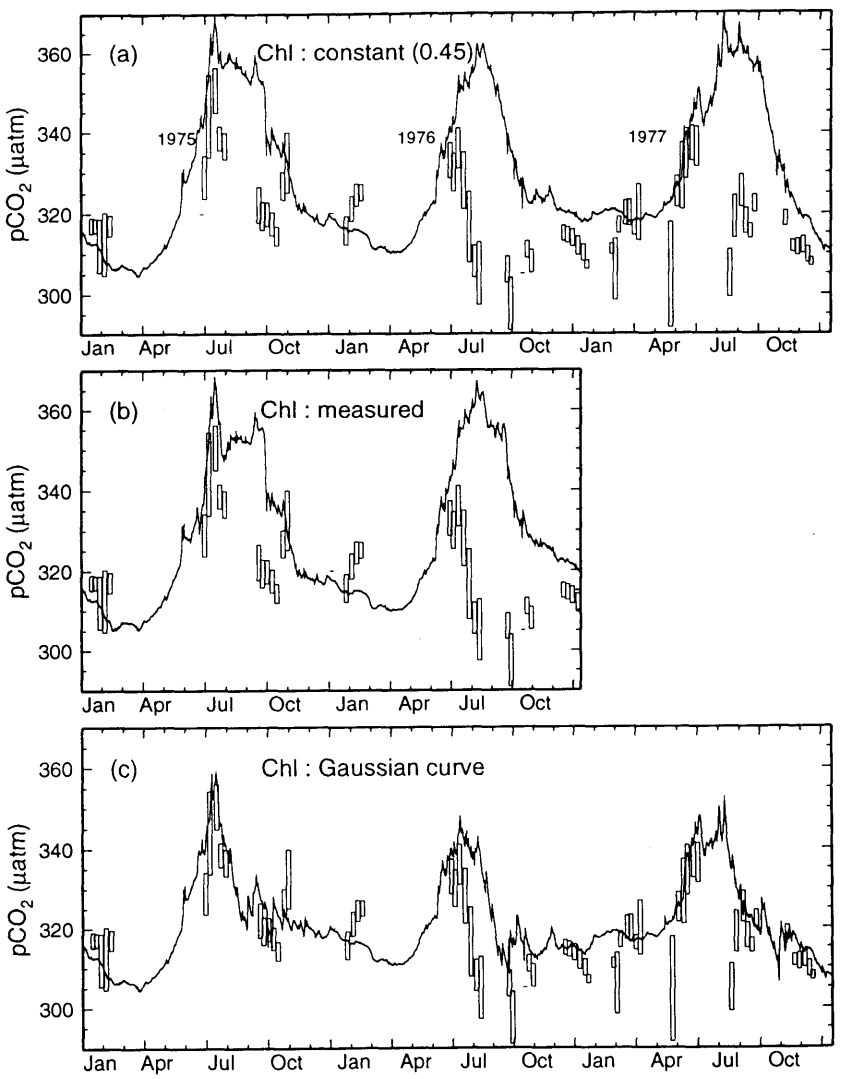

Fig. 7. Mixed-layer pCO_2 obtained when the model is fed (a) with a constant Chl concentration throughout the year (0.45 mg(Chl) m^{-3}), (b) with the Chl cycle interpolated from the measured Chl concentrations, (c) with the mean Gaussian cycle for Chl.

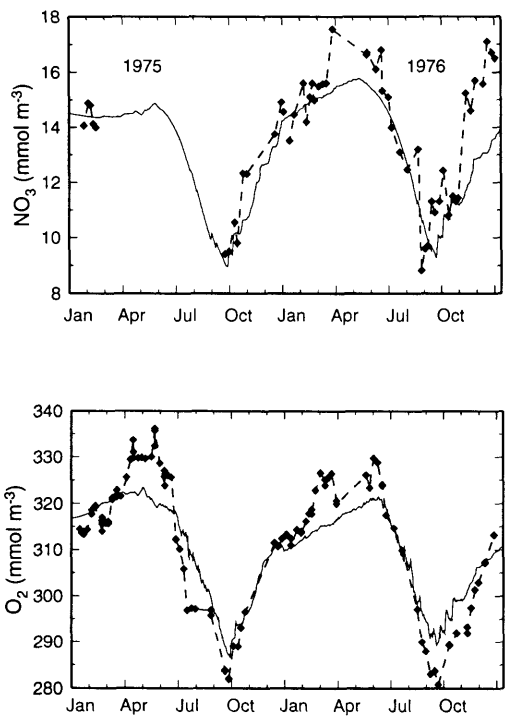

Fig. 8. Measured nitrate and oxygen concentrations (diamonds) within the mixed-layer (no data in 1977), and as computed when the model is fed with the Gaussian cycle for Chl (solid curves).

net oxygen production (3.9 mol $O_2\,m^{-2}\,y^{-1}$ here, versus 2.8–4.2 mol $O_2\,m^{-2}\,y^{-1}$ in Emerson et al., 1991). Interestingly the net uptake of carbon seems to occur exclusively within the mixed layer at OWSP, as the consumption below this layer is on average equal to the fixation. The mean annual ratio of the net C uptake (i.e., $P-R$) to the primary production (P) is about 0.5 when considering only the mixed-layer domain, instead of 0.36 adopted for the whole productive layer.

Despite possible outgassing in July and August, Station Papa is ultimately a sink for CO_2 (see Fig. 9a) and the entering flux is estimated to be on average 0.62 mol $CO_2\,m^{-2}\,y^{-1}$, i.e., slightly less than the value (0.70) proposed by Wong and Chan (1991). It is a source for O_2 and the annual outgassing flux resulting from the model is on average 2.3 mol $O_2\,m^{-2}\,y^{-1}$. From their model, Thomas et al. (1993) estimated the O_2 outgassing flux to be in the range 0.2 to 2 mol $O_2\,m^{-2}\,y^{-1}$, while Emerson et al. (1991) deduced a value as high as 12 mol $O_2\,m^{-2}\,y^{-1}$ from oxygen mass balance calculations by considering summer data only. A great uncertainty still remains about the magnitude of the oxygen exchange at the air-sea interface. The downward export of the biologically-produced O_2 was estimated between 0 and 4 mol$O_2\,m^{-2}\,y^{-1}$ by Emerson et al. (1991), to be compared to 2.6 mol $O_2\,m^{-2}\,y^{-1}$, from the present simulation. For nitrate, Miller et al. (1991) calculated an upward flux through the halocline of 2.2 mmol $NO_3\,m^{-2}\,d^{-1}$, slightly above the present estimate, 1.2 mmol $NO_3\,m^{-2}\,d^{-1}$ (0.43 mol $NO_3\,m^{-2}\,y^{-1}$).

The computed fluxes lead to weakly unbalanced annual budgets. The residuals, however, are very small with respect to the involved fluxes. They are also comparable in magnitude to those derived from measurements. For example, the net carbon uptake by biota, supported by the capture of atmospheric CO_2 (20%), and by the upward CO_2 flux (80%), remains slightly unbalanced. With respect to O_2, the deficits are -1.7 and -0.4 mol $O_2\,m^{-2}\,y^{-1}$ for 1975 and 1976 respectively (Table 3), in agreement with the field data (-3.3 and -0.33 respectively). The amount of O_2 exported towards the atmosphere and towards the deep layers (45% and 55%, respectively), would be slightly larger for the three years than the net O_2 production by phytoplankton. A different partitioning when dealing with O_2 and CO_2 is conceivably due to the fact that O_2 is more rapidly exchanged through the air-sea interface than CO_2. The field data would lead to a gain of 53 mmol $NO_3\,m^{-2}\,y^{-1}$ at the end of 1975, while (in absence of advection) the model produces a loss of -44 mmol $NO_3\,m^{-2}\,y^{-1}$. In the simulation, the upward flux of NO_3 (386 mmol $NO_3\,m^{-2}\,y^{-1}$) nearly makes up for the net uptake by phytoplankton (430 mmol $NO_3\,m^{-2}\,y^{-1}$).

It is worth noting that the upward CO_2 and NO_3 fluxes are not linked by the Redfield ratio (i.e., $106/15 = 7.06$). Their ratio is smaller (about 5.2) because the C uptake by phytoplankton, in contrast with the nitrate uptake, is not only balanced by diffusivity, but also by air-sea exchange. This is confirmed by forming the ratio of the sum of the CO_2 upward flux plus air-sea exchange to the upward NO_3 flux, that is reset to the nominal value 7.

Table 3. *Carbon, oxygen and nitrate fluxes obtained via the model, when it is fed with the Gaussian cycle for chlorophyll*

		1975		1976		1977		mean	
		(mmol $m^{-2} y^{-1}$)	(gC $m^{-2} y^{-1}$)	(mmol $m^{-2} y^{-1}$)	(gC $m^{-2} y^{-1}$)	(mmol $m^{-2} y^{-1}$)	(gC $m^{-2} y^{-1}$)	(mmol $m^{-2} y^{-1}$)	(gC $m^{-2} y^{-1}$)
C (CO_2)	$-P$	−8430	−101	−8590	−103	−8865	−106.4	−8628	−103.5
	$-P+R$ mixed layer	−3170	−38	−3060	−36.7	−2890	−34.7	−3040	−36.5
	$-P+R$ "stratified"	+200	+2.4	+40	+0.5	−280	−3.4	−13	−0.15
	$-P+R$ total	−2970	−35.7	−3020	−36.2	−3170	−38	−3053	−36.7
	upward flux	+2730		+1880		+2230		+2280	
	air-sea exchange	+560		+630		+680		+623	
	budget	+320		−510		−260		−150	
O_2	$P-R$ mixed layer	+3820		+3680		+3485		+3662	
	$P-R$ "stratified"	+45		+260		+640		+315	
	$P-R$ total	+3865		+3940		+4125		+3977	
	upward flux	−2600		−2410		−2890		−2633	
	air-sea exchange	−3000		−1950		−1925		−2292	
	budget	−1735		−420		−690		−948	
NO_3	uptake mixed layer	−310		−300		−280		−297	
	uptake "stratified"	−120		−140		−170		−143	
	total uptake	−430		−440		−450		−440	
	upward flux	+386		+405		+530		+440	
	budget	−44		−35		+80		+0	

Units are mmol $m^{-2} y^{-1}$ and also gC $m^{-2} y^{-1}$ for carbon fluxes. These values are for the water column extending from 0 to 300 m depth, divided into "mixed layer" and "stratified", below the mixed layer. They are negative if they represent a loss for the water column. For CO_2, $-P+R$ represents the net C uptake. For O_2, $P-R$ is the net O_2 production. In the last column, the budgets are averaged over the three years.

2.7. *Relative importance of the various processes in governing the ΣCO_2 and pCO_2 evolution*

The physical and biological processes, regulating the mixed-layer ΣCO_2 content with various and time-dependent efficiencies, can be separately analysed through the model. Unlike pCO_2, ΣCO_2 does not depend on temperature variations, and the three-year mean C-fluxes estimates in Table 3 (last column) show that biological activity ($P - R$) is the main factor controlling ΣCO_2, and that the upward flux and then the air-sea exchange follow in order of decreasing importances. In Garçon et al. (1992), the three processes were found to equally contribute to the ΣCO_2 change at OWSP, for the years 1971 and 1972. Their method, however, was quite different, as they successively introduced the various processes in different

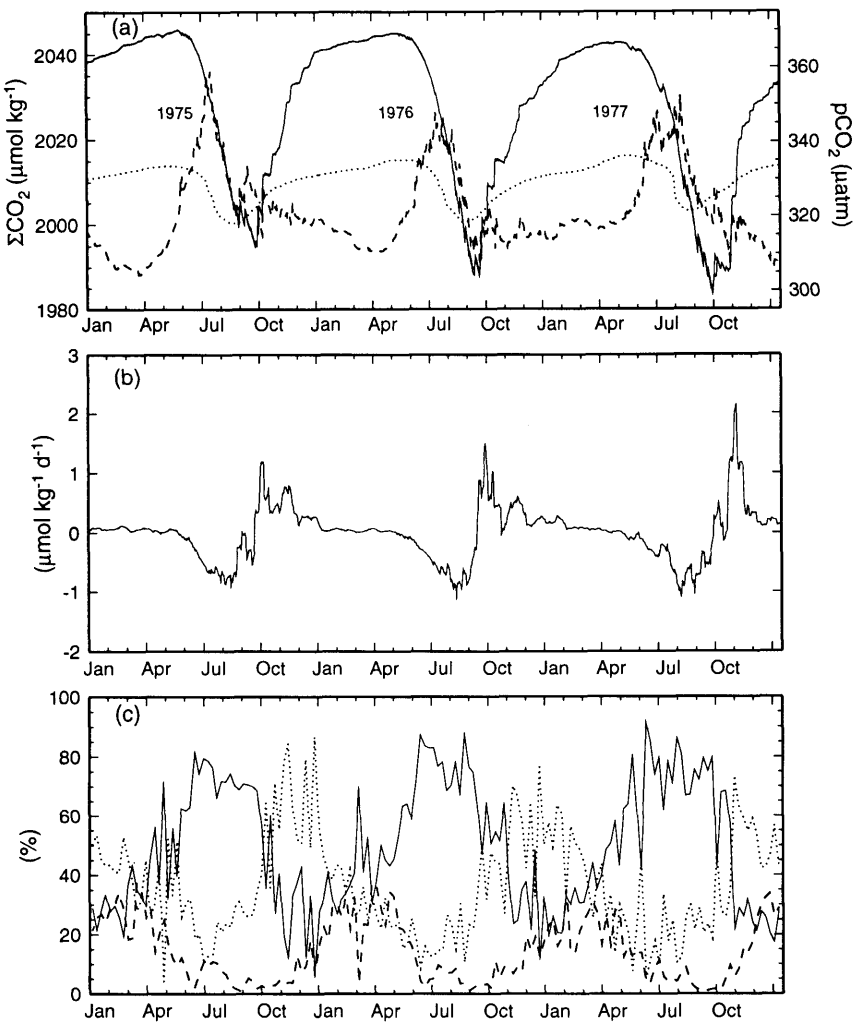

Fig. 9. (a) Computed annual courses of the ΣCO_2 content within the mixed layer, when the present model is fed with the Chl Gaussian cycle; the pCO_2 cycle (from Fig. 7c) is shown again for comparison (dashed curve), as well as the evolution of the atmospheric pCO_2 (dotted curve). (b) the derivative of ΣCO_2, expressed as daily change. (c) Relative importance (as %), in changing the mixed-layer ΣCO_2 content, of biology (solid line), eddy diffusivity plus entrainment (dotted line), and air-sea exchange (dashed line).

simulations. This general pattern must be nuanced when the annual courses are considered (Fig. 9c). During winter, air-sea exchange, biological activity, and eddy diffusivity plus entrainment are of comparable importance; the ΣCO_2 change at this period, however, is reduced (Fig. 9b). The divergence starts in spring and is maximum in july, when the biological activity is responsible for up to 80% of the negative ΣCO_2 change. From July to October, the ΔpCO_2 is close to zero, and the air-sea exchange is almost annihilated. The relative rôle of diffusivity plus entrainment is approximately the reversed image of that of biology; it becomes progressively preponderant in autumn, when the ΣCO_2 change is positive, and is a consequence of the mixed-layer deepening. In general, any drawdown in the ΣCO_2 content due to the biological activity within the mixed layer is thereafter compensated by an upward flux of CO_2-rich waters and by a CO_2 invasion from the atmosphere (when OWSP is a sink for atmospheric CO_2). The biologically and the physically induced ΣCO_2 variations show opposite variations with a phase lag of 6 months. Because the wind speed seasonality is weak and the temperature effects on the CO_2-transfer velocity and CO_2 solubility nearly cancel each other (leading to an almost constant gas-exchange coefficient), the air-sea exchange at OWSP is almost exclusively sized by the ΔpCO_2, whatever the physical environment. During winter, eddy diffusivity has never a strong impact on ΣCO_2 at station Papa, for at least two reasons (i) the mixed layer is clamped by the permanent halocline, which acts as a barrier to diffusive exchanges, and (ii) the ΣCO_2 gradient between mixed layer and deeper waters is weak.

It is noteworthy that the biologically-mediated variations in ΣCO_2, O_2 or NO_3 within the deep, stratified, layers, play a decisive role in determining the mixed-layer concentrations. Indeed, non negligible O_2 production, CO_2 and NO_3 uptake occur in these layers, able by this way to affect the exchange rates with the mixed layer. If biology was hypothetically made inoperative inside the stratified domain, the main consequence would be a reinforcement of the air-sea exchanges, by about 10% and 40%, for CO_2 and O_2 respectively. The pCO_2 also rapidly would diverge from the field data, for example exceeding by 20 μatm the observed level in summer 1977. These remarks remain valid when the productive domain ($1.5Z_e$) is restricted to the euphotic zone (Z_e).

In addition to the changes in ΣCO_2, the pCO_2 reflects the influence of the SST variations (Figs. 9a and 3a). The divergences between the pCO_2 and ΣCO_2 evolutions originates from the varying weights of the thermodynamics (on pCO_2), and of biological activity and eddy diffusivity (on ΣCO_2). For example, during winter 1975, pCO_2 experiences a minimum while ΣCO_2 is almost constant. After opposite evolution in spring, both pCO_2 and ΣCO_2 are simultaneously declining in summer. During this period, however, the SST increase conflicts with the simultaneous ΣCO_2 decrease, and the pCO_2 drawdown is accordingly reduced with respect to that expected for constant temperature. In autumn, the sharp increase in ΣCO_2 (due to entrainment) is in no way reflected by a parallel pCO_2 change, because SST is markedly decreasing at this time of the year.

3. A simplified version of the model

When validating the complete model at station Papa, the biological compartment was finally fed with an imposed Chl cycle in the upper layer, and the vertical pigment profiles were inferred from this single piece of information. Similar inputs will be available for the future use of the model in conjunction with satellite-derived information. In contrast, the physical segment was driven by the three-hourly meteorological records at station Papa. Such detailed inputs will obviously be lacking for studies at large scale. Even if, in principle, remotely-sensed data about SST, wind and irradiation will be available, it will remain out of reach to retrieve everywhere in the ocean the evolution of the mixed layer with an accuracy comparable to that obtainable when using meteorological records. In this section, the EKE sub-model is therefore voluntarily abandoned (a sensitivity study to the mixed layer representation will be presented later on). It is admitted that the annual courses of the mixed-layer depth and temperature, and of the eddy diffusivities, will be prescribed, by relying on climatological information, or outlined by using intermittent space observations. This simplified version is described and operated below, in a comparison exercise with the modelling approach developed by Taylor et al. (1991).

3.1. Comparison with Taylor et al.'s results

The climatological situations studied by Taylor et al. (1991) are revisited; they are located at latitudes 0, 35, 47 and 60° N in the Atlantic Ocean. In the Taylor et al.'s study, thereafter denoted TL, attention was focused on the development of the spring bloom, and on its impact on ΣCO_2 within the upper layer. The pCO_2 and ΣCO_2 annual cycles produced by their model and by the simplified version of the present one are compared.

In TL, the annual changes in the physical structure of the upper oceanic layers were imposed and three boxes (mixed layer, thermocline and deep waters) were considered. The annual courses of the mixed-layer depth and temperature are taken from TL to drive the present model. Associated with the mixed-layer minimum depth, a minimum eddy diffusivity value is adopted ($K_{z,\min} = 10^{-5}\ m^2\ s^{-1}$) at the base of this layer. The actual K_z coefficient for a given day is scaled by the mixed-layer depth, according to $K_z = K_{z,\min}\ (Z_{ml}/25)^{1.5}$, as done in TL. Inside the pycnocline or in the deep layers beneath, K_z is given the constant values 10^{-5} or $3 \cdot 10^{-5}\ m^2\ s^{-1}$, respectively. Salinity is kept constant throughout the year, at 37, 37, 35.5, and 33 psu.

The temporal evolution of the phytoplankton biomass was modeled in TL, within a single-species and single-nutrient (nitrate) system. The annual cycles for pigments, resulting from TL's modelling, are directly used as inputs to drive the present model. The f-ratio is not involved in TL. Concerning the present model, extrema for the f-ratio (0.2–0.7) are adopted in such a way that the mean annual f-value is 0.3, a value generally believed to be typical of the open ocean (Platt et al., 1989), except for the equatorial station, where a constant f value of 0.1, probably more realistic, is adopted. The annual course of the f-ratio is assumed to mimic that of Chl, with a maximum coinciding with the spring bloom, and a minimum occuring in summer. A sensitivity study, with respect to the mean f-ratio, and to the mixed-layer annual course, will be presented later on.

Annual means of the cloudiness index, namely 5, 5.5, 6 and 6.5 okta for the latitudes in question, were taken in a cloud cover atlas (NCAR, 1988) in order to estimate the incident radiation. In TL a constant piston velocity for air-sea CO_2 gas-exchange ($4.8\ m\ d^{-1}$) was assumed. According to the mean temperatures at each station, such a value would correspond to constant wind speeds of 8, 10, 12, and $13\ m\ s^{-1}$. The ΣCO_2 vertical profiles used as initial conditions were built from the ΣCO_2 values choosen by TL for the upper box and for the deep reservoir. Salinity is kept constant, and the biologically-induced variations in TA are not taken into account. Surface values of TA were selected, and kept constant throughout the year, in such a way that, when combined with the ΣCO_2, SST and salinity, they lead to the pCO_2 level adopted by TL at the beginning of each of their simulation.

The qualitative agreement between the pCO_2 and ΣCO_2 annual cycles, as obtained with the present model, and those of TL, is good (Fig. 10), with simultaneous pCO_2 rises and falls. At the equator, the pCO_2 (not displayed) is nearly constant throughout the year, around 370 μatm. At the other locations, and especially at 47° N, however, the amplitude of the pCO_2 drawdown due to the phytoplankton bloom, or the post-bloom pCO_2 rise, differ in the two models. Differences in parameterising the net effect of the plankton community on ΣCO_2 and the diffusive exchanges are at the origin of these divergences. During the maximum blooming at 47° N, and given the surface Chl value ($6.5\ mg\ Chl\ m^{-3}$, adopted from TL), the total Chl content over the mixed layer-plus-thermocline domain in TL is about twice the total Chl content estimated in the present model, where the depth of integration is that of the productive layer. This difference is mainly responsible for the variable impact of the spring bloom on the pCO_2 in the two models. By tuning somewhat arbitrarily these parameters, it could have been possible to reach a better agreement, which actually has no particular significance per se.

As previously underlined by TL, these academic simulations demonstrate that the effect of algal activity on ΣCO_2 is increasing with increasing latitude. At 35° N, the signal is essentially controlled by the SST cycle, while at 60° N the phytoplankton bloom has a dominant influence on the pCO_2 level. The concordance between the results of both models demonstrates that at least the general trends of the carbon cycling within the upper ocean can be understood, even if not easily predicted in a quantitative way. This understand-

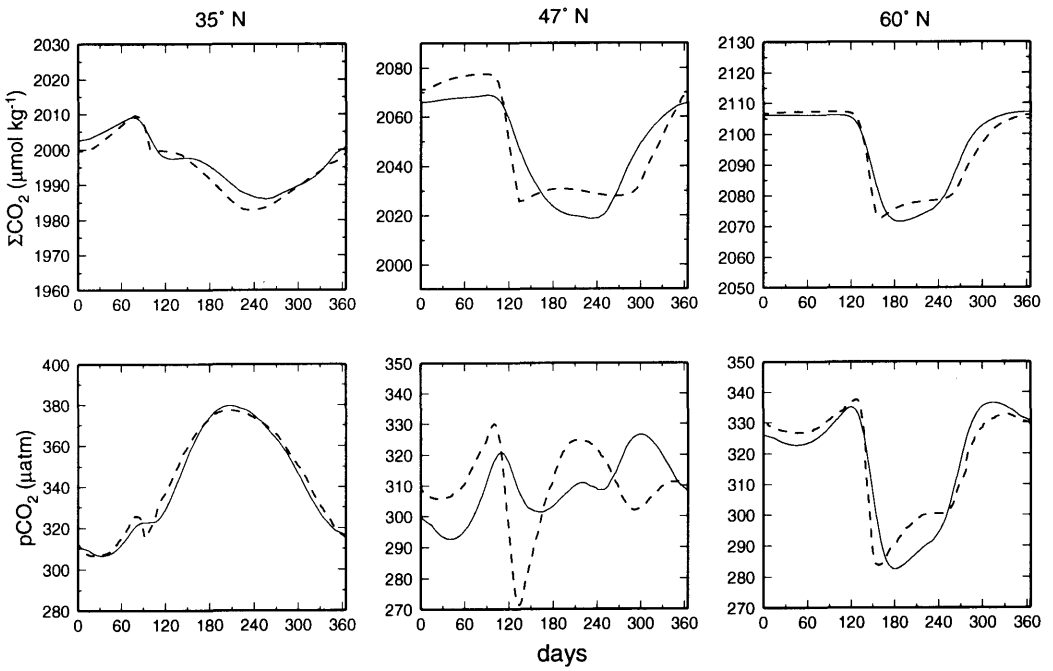

Fig. 10. Annual courses of ΣCO_2 (top) and pCO_2 (bottom) for the "case-stations" at 35, 47 and 60° N. Dotted curves are the cycles as obtained by Taylor et al. (1991), and solid curves are those resulting from the present modelling.

ing allows to examine the reliability of methods which make use of Chl and SST as predictors of the pCO_2 evolution.

3.2. *SST and Chl as proxies for pCO_2*

Various correlations have been occasionally detected between pCO_2 and SST or Chl concentration within the upper layer of the ocean (Takahashi et al., 1983; Watson et al., 1991). By using such correlations, SST and Chl, as detectable from space, could help in constructing large-scale pCO_2 fields. Once combined with CO_2 gas-transfer coefficient derived from wind scatterometry, such pCO_2 maps would allow the air-sea CO_2 flux to be inferred at large scale (Etcheto and Merlivat, 1988; Thomas et al., 1988; Erickson, 1989; Etcheto et al., 1991). Tans et al. (1990), for instance, attempted to map the ΔpCO_2, between ocean and atmosphere, by using relationships between ocean SST and pCO_2, made dependent on latitude but not on the season. The possibility of extending in space and time such local and episodic correlations remain an open question.

The pCO_2 annual cycles at the three sites are plotted as a function of Chl or SST (Fig. 11). The pCO_2 annual cycle obtained at station Papa (for 1975) is also shown for comparison. The increasing impact of the spring bloom on pCO_2 with increasing latitude is clearly shown by Fig. 11. In response to the bloom, the pCO_2 change is about 4, 25, and 40 μatm at 35, 47, and 60° N respectively, and definitely not sized by the magnitude of the bloom itself, if expressed in terms of Chl increase (namely 2, 5, and 4 mg(Chl) m^{-3} at 35, 47, and 60° N). In a given location, at 47° N for instance, pCO_2 can remain almost constant while Chl is rapidly increasing (onset of the bloom), or decreasing (post-bloom conditions), even if the mean pCO_2 level differ by about 20 μatm before and after the bloom. Conversely, at constant Chl concentration (from summer to autumn), pCO_2 is markedly increasing. At 35° N, the absence of correlation is even more marked as the Chl change is in no way refelected by a pCO_2 variation; at this latitude the pCO_2 cycle is dominated by the temperature evolution.

Concerning the pCO_2-SST relationships the situation is equally complex. According to the

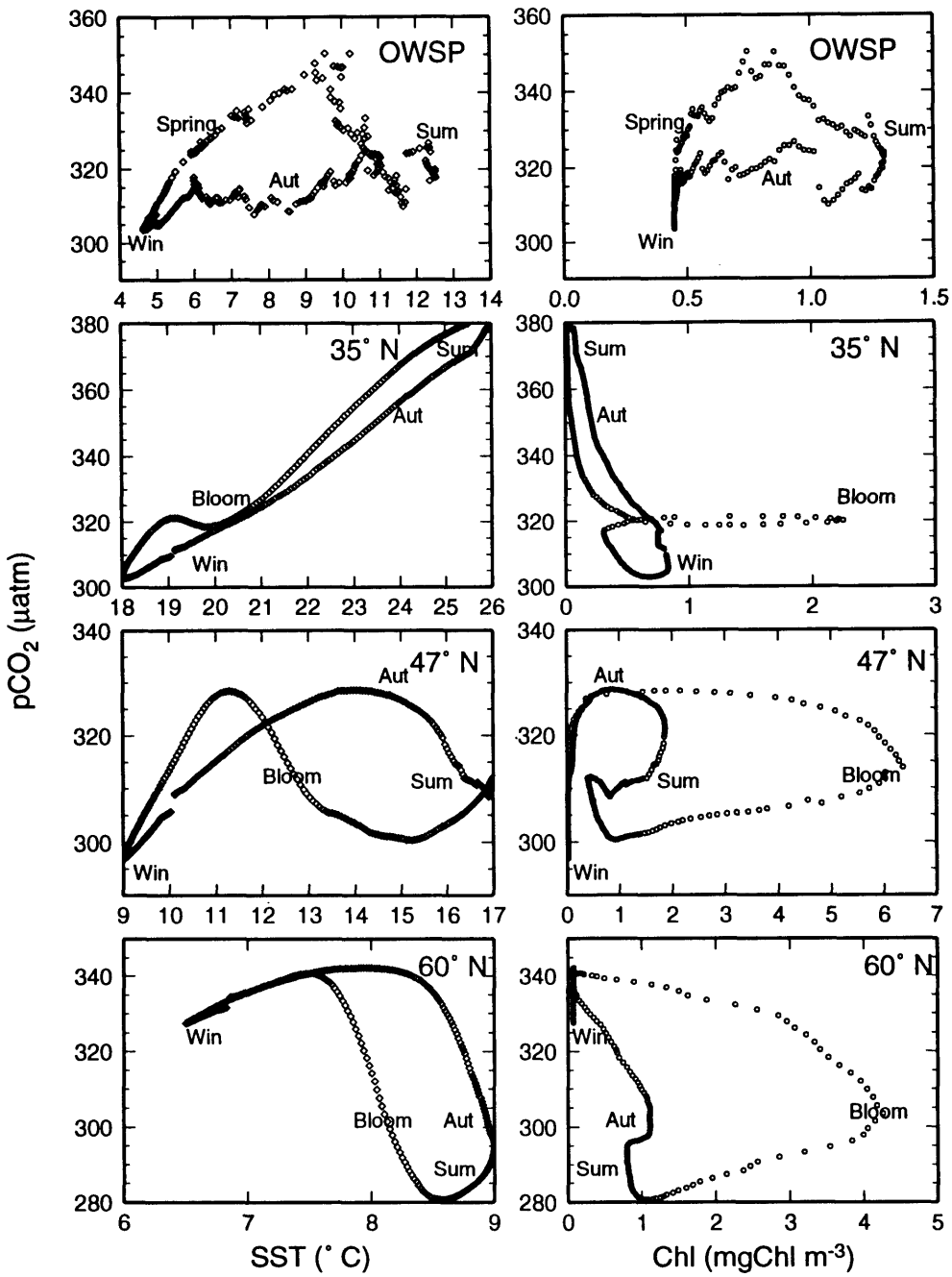

Fig. 11. Mixed-layer pCO_2 obtained via the simplified version of the present model, versus temperature (left column) and sea-surface Chl concentration (right column), for the same stations as in Fig. 10, and also for station P (upper plot, for the year 1975). The complete annual courses are represented and the labels "Win", "Bloom", "Sum" and "Aut" stand respectively for winter, bloom, summer and automn periods.

season, the pCO_2 change can be either correlated (from autumn to winter at 47°N, for instance) or anti-correlated (bloom period) with the SST evolution. Such conclusions cannot be generalised because they depend on latitude, and also on the oceanic area. For example, the pCO_2-SST plots, at station Papa (50°N in the Pacific) and at the case-station at 47°N (in the Atlantic), do not show the same patterns.

These rather complex relationships emphasise that Chl and SST are ambiguous proxies of the evolution of pCO_2 at a given site, and illustrate the importance of the previous history of the water body in the determination of its pCO_2 level at a given instant. Although the Chl concentration is believed as being an essential parameter for the upper-ocean CO_2 modulation, its instantaneous and local knowledge is insufficient to infer a reliable value of the upper-ocean pCO_2 (Yoder et al., 1993). The same conclusion is obviously valid for the SST.

These pessimistic conclusions are inevitable when trying to extract from the entire annual cycles of the pCO_2, SST and Chl at a given site some reliable and univocal relationships. The situation is different when larger spaces are considered, and if the evolution of the SST or Chl fields can be monitored. Various correlations between the seasonal values of the pCO_2, SST and Chl actually exist at regional scale (Metzl et al., 1991; Poisson et al., 1993); in an implicit way they integrate the previous evolution of the system. On such seasonally-dependent relationships, derived from field data, rests the development of methods to reconstruct continuous pCO_2 fields by using climatological (or, in the future, remotely-sensed) SST and Chl fields.

4. Sensitivity studies

Prior to testing the model sensitivity to modified parameterisations, the internal consistency of the computations has been checked. The daily pCO_2 is permanently generated from the daily values of ΣCO_2 and TA. The relative variations of pCO_2 can be expanded by using the partial derivatives

$$\frac{dpCO_2}{pCO_2} = \sum_1^4 \left(\frac{\partial pCO_2}{pCO_2} \frac{1}{\partial X} \right) dX,$$

where X is either SST, ΣCO_2, TA, or salinity (practically, at station Papa, TA and salinity are not involved, and are kept at 2215 μequ kg^{-1} and 32.8 psu, respectively). To obtain the numerical value of each partial derivative, the other parameter must be kept constant. They are given their mean value over the three years considered, namely 8°C for SST and 2025 μmol kg^{-1} for ΣCO_2. With these values, the partial derivatives turn out to be $+0.043\ (°C)^{-1}$ and $+0.0056\ (\mu mol\ kg^{-1})^{-1}$. When combined with the daily variations in SST and ΣCO_2, obtained through the model, and by summing the two contributions, new (actually less accurate) pCO_2 values are obtained. They agree with the accurate values within $\pm 2\ \mu$atm, and confirm the numerical competence of the code.

Various sensitivity experiments are thereafter presented. They concern the representation of the Chl cycle and of the mixed-layer depth, the impact of the prescribed values, namely the f and the C-to-Chl ratio. They are carried out for station Papa and also for the "case-stations" examined in the previous section.

4.1. The chlorophyll representation in the model

The first sensitivity test involving the Chl representation in the model has been already described; it has led to the adoption of a Gaussian cycle (Fig. 4a). With respect to this choice, the impact of modified Gaussian cycles was tested. In a first trial, the same Chl cycle was just shifted by ± 10 days, resulting in minute effects on the chemical evolution and annual budgets. Widening the peak, covering 250 days instead of 150, enhances the new production by 12%; correlatively the CO_2 entering flux is raised by 37%. The sensitivity to more pronounced blooms, with the same Gaussian profile peaking at 2.0 instead of 1.6 mg Chl m^{-3}, was also studied. As expected, the new production is enhanced by 7%, whereas the CO_2 invasion is increased by 20%. From June to October, the mixed-layer pCO_2 is depressed by about 5–10 μatm (wider peak) or about 5 μatm (higher peak). In all these experiments, the oxygen budget was never notably modified, as a consequence of the rapid response of the outgassing (increased by up to +25%). The response inside the inorganic carbon compartment, when the physical constraints are practically unchanged (apart from the heating rate), are not linearly related to the

changes imposed to the algal biomass. If still needed, these sensitivity studies demonstrate that in any model a good Chl cycle representation, and hence the availability of a continuous Chl information, are essential.

The impact of the vertical pigment distribution is also tested, by replacing the non-uniform vertical profiles by uniform Chl profiles throughout the year. The resulting pCO_2 cycles are nearly unchanged at station Papa and for the case-stations previously studied, except at 47° N in summer, where a local enhancement of the pCO_2 (by 5 μatm) lasts two months. The resulting C fluxes are not significantly affected (within ±2%) at 47° N, 60° N and at station Papa. In contrast, changes are notable at the Equator and at 35° N. At the equatorial station, the deep chlorophyll maximum is permanently located at about 120 meters; if it is ignored (what is irrealistic), the integrated Chl content within the productive layer is decreased by 65% and primary production in the deep layers is halved. The annual column-integrated primary production is decreased by 40%, and more CO_2 is thus brought from below toward the mixed layer (+40%). The CO_2 air-sea exchange is, however, nearly unchanged, as a consequence of an increased biological consumption in the upper layers (the recycling term, R, being decreased). At the 35° N station, deep chlorophyll maxima are only characteristic of summer; if they are ignored, similar changes are observed than at the equatorial station, with however a lesser amplitude. As expected, uniform vertical profiles are not representative for the low latitude stations, where the stratification is intense, the upper-layer chlorophyll concentration low, and the deep chlorophyll maximum well developed.

4.2. The f-ratio and the C-to-Chl ratio

The Gaussian cycle being fixed, it remains to examine the effect of two other ecological parameters, the mean f-ratio and the C-to-Chl ratio. Incidentally, if at station Papa f is given the value 0.30, instead of 0.36, the deficit that appeared in the carbon budget over the three years considered, is annihilated. This relatively minor adjustment confirms that the deficit found in the annual budgets (Table 3) is not really significant and also suggests that the response of the model is very sensitive to the f value. Therefore, two extreme values have been tested, namely 0.18 and 0.54 (±50% around the mean), even if they are irrealistic for OWSP. The new pCO_2 and NO_3 cycles rapidly diverge from the field data. When f is 0.18, the upward fluxes are modified by about −12, +6 and −23%, for ΣCO_2, O_2 and NO_3 respectively. These changes turn out to be +13, −6 and +23% when f is 0.54. The CO_2 flux due to gas-exchange increases by 130% if f is 0.54 (by 93% for O_2), and becomes an outgassing (or decreases by 90% for O_2) when f is 0.18. Interestingly, the difference expected in the carbon budget, as a consequence of the change in new production (with respect to the basic case with $f = 0.36$), is almost entirely obliterated (actually by up to 80%). This quasi-compensation is inequally shared by an increase of the dissolution process (+130%) and of the upward transport (+13%). The disproportion is even more accentuated for oxygen. When O_2 is in excess inside the mixed layer, the compensation only results from a 93% increase of the outgassing.

In another numerical experiment at station Papa, the f-ratio was made varying according to the four mean field estimates of Wheeler and Kokkinakis (1990), as shown on Fig. 4b. By this way, the mean annual value of f (0.36) is respected, whereas the f_d values are allowed to fluctuate between 0.4 in winter and 0.25 in summer. Changes in the pCO_2, O_2 or NO_3 annual cycles and budgets are minor. Thus, some uncertainties in the annual course of the f-ratio would not preclude a proper estimate of the fluxes, provided that the relevant mean annual value of f is respected. A similar experiment was made on the "case-stations", by assuming a constant (0.3) f-ratio throughout the year, instead of making it varying with the Chl concentration. Significant changes are obtained in the pCO_2 annual cycles. The above conclusion is to be nuanced for stations where the annual cycle for f would be characterised by pronounced variations. A test has been also carried out on the "case-stations", by increasing or decreasing the mean f-values by 0.1 (extrema become then 0.1–0.6 or 0.3–0.8, instead of 0.2–0.7). The pCO_2 and ΣCO_2 cycles are also significantly altered, the air-sea fluxes being the most affected by the change in f (for example, the CO_2 entering flux decreases by up to 50% at 35° N, when f decreases). These results from the sensitivity studies emphasize the crucial buffer role of the atmosphere, able to regulate efficiently the upper-

ocean CO_2 and O_2 content, when modified by a change in the biological pump functioning. This conclusion, however, could be invalidated, for example at a station where the wind speed is much lower than at station Papa. The situation for nitrate is obviously different; when changing f, the unbalanced budget is only partly compensated (50%) by a modified upward transport.

The C-to-Chl ratio is by far more uncertain. A test was made by considering a constant higher value, i.e., 100 instead of 53, and in a second run, the C-to-Chl ratio was given a sinusoidal pattern, as suggested for station Papa by McAllister (1969)

$$\text{C-to-Chl} = 30 - 15\cos(2\pi(\text{day} - 15)/365)$$

and thus varies from 15 (winter) to 45 (summer). Surprisingly, very small, unsignificant, changes are observed in both cases, either in the annual cycles or for the annual budgets. This weak influence of the C-to-Chl ratio is inherent in the method used here to calculate the rates of local recycling and export of primary production. Indeed, a careful examination of this method shows that a modification of the C-to-Chl ratio leads to opposite and compensatory effects.

4.3. *Short-term events in the annual course of the mixed-layer depth*

The eddy diffusivity coefficient at the base of the mixed layer, $K_{z,\mathrm{ml}}$, is sensitive to the physical constraints. Thus, prior to testing the sensitivity of the model to the short-term changes in the physical forcing, a test is carried out on the value of $K_{z,\mathrm{ml}}$. The exchange between the mixed layer, which consists of a unique box, and the underlaying waters is entirely ruled by the $K_{z,\mathrm{ml}}$ value, and a high sensitivity of the model to this parameter is expected (note that it is not specific to the present model, but is inherent to any simulation of the mixed layer as a unique box). By increasing $K_{z,\mathrm{ml}}$ by 50% throughout the three years of simulation at station Papa, the mean yearly upward ΣCO_2 flux is raised by 20%, while the CO_2 entering flux is decreased by 50%, as a consequence of the enhancement of the mean pCO_2 level (by about 10 μatm in 1977). The impact of an opposite change in $K_{z,\mathrm{ml}}$ (-50%) is greater, the above percentages becoming -30% and $+75$% respectively, and the mean pCO_2 level is lowered by about 10 μatm in 1977. These two tests also produce significant changes in the O_2 and NO_3 fluxes, the O_2 concentration being however practically unchanged, mainly as a consequence of the efficient air-sea O_2 transfer.

The sensitivity of the model to the mixed-layer representation has also to be envisaged. To simulate a kind of "climatological" physical forcing, monthly averages have been computed for the mixed-layer depth and temperature and for the eddy diffusivities obtained through the EKE model. Daily values are then re-interpolated within this monthly values and short-term variations are thus totally smoothed. The model is run with these smoothed values over the three years (and by using again the Gaussian Chl cycle and $f = 0.36$). The pCO_2 variations and the mean pCO_2 level are approximately reproduced during the first 21 months (results not shown). After this period, a serious drift starts, and the model thereafter totally fails in reproducing the pCO_2. This result emphasizes the importance of the short-term variation (within a few days) of the physical constraints. The permanent succession of mixing and stratification events (see Fig. 3b) is able to modify the mixed-layer pCO_2, either by bringing up ΣCO_2-rich deep waters and by simultaneously cooling the sea-surface waters, or by heating and stabilising the upper layers. Ignoring such events introduces artifactual offsets in the simulated ΣCO_2 and pCO_2, as compared with the corresponding measurements, which can, in a non predictable way, either compensate or accumulate during the successive days of the simulation. The reproduction of the O_2 and NO_3 annual cycles is clearly less sensible to the smoothing of the physical forcing, their seasonal evolutions being well simulated, even if the short-term variations are not reproduced. In the case of O_2, this is probably a consequence of the more rapid exchange with the atmosphere, as compared to CO_2, allowing the excesses or deficits in the mixed layer to be rapidly compensated. It is likely that the independance of NO_3 upon temperature is responsible for its lesser sensibility to the present smoothing of the physical constraints.

The same test has been also carried out on the three "case-stations" examined in the previous section, relatively to the prescribed extrema. The mixed-layer depth was increased or decreased, by 10 meters for the summer minimum, and by 50 m for the winter maximum. These modifications result again in significant changes in the ΣCO_2 and

pCO_2 annual cycles. Changes by up to $\pm 50\%$ are observed for the ΣCO_2 upward flux and the CO_2 air-sea exchange. These modifications, however, never reverse the direction of the carbon fluxes. These tests show that, beside the short-term variations in mixed-layer depth, the depths attained during the winter overturn and also the thickness of the mixed layer during the stratified period are equally important parameters. They determine to a large extent the ΣCO_2 content of the water mass in winter, and particularly before the onset of the spring bloom.

5. Conclusion

The successful validation of the full model at station Papa is encouraging. In addition, a simplified version of the model has produced pCO_2 cycles in agreement with those obtained by Taylor et al. (1991) in various climatic environments.

An important characteristic of the present model is to derive the impact of the biological activity on the ΣCO_2 only from the chlorophyll concentration at the sea surface. The sensitivity tests emphasize the importance of a good representation in the model of the chlorophyll annual cycle, and even of short-term events, particularly in summer time. This sensitivity, however, does not preclude the future use of the model at large scale, as ocean colour sensors will provide the necessary information. For example, the SeaWIFS instrument (Hooker et al., 1992) will provide a global earth coverage each three days, with an increased accuracy for the pigment determination. Furthermore, at least two other ocean colour sensors (the Japanese OCTS, and the European POLDER instruments, Deschamps et al., 1990) will be simultaneously operating. From the remotely-sensed Chl concentrations, the vertical pigment distribution can be inferred by using statistical relationships, as done in the present study. The sensitivity tests have confirmed that the vertical pigment structure is, as expected, particularly important for the ΣCO_2 budget in the oligotrophic ocean, where deep chlorophyll maxima are well developed. More crucial is the adoption of a relevant mean value for the f-ratio, even if some uncertainties in its annual course have not a dramatic impact on the pCO_2 evolution. The link between this ratio and the total primary production (Eppley and Peterson, 1979), although somewhat circular, is certainly a guideline, as could be also a rough estimate of the nutrient level from the temperature field (Kamykowski and Zentara, 1986). Several attempts to assess the new production were made along this line (Dugdale et al., 1989; Sathyendranath et al., 1991) and likely have to be generalised.

Improvements can be made, following two somewhat diverging directions, in correspondance with two possible applications. One improvement could be a complexification of the model in view of describing in every detail the pCO_2 evolution at a given station or test site, particularly well documented (a JGOFS permanent station for instance). The hypothesis of instantaneous and perfect homogeneisation within the mixed layer can be relaxed. There is also no particular problem in keeping the nycthemeral cycles, instead of averaging over a 24-h period. The physiological parameters (specific absorption, parameters of the light-photosynthesis curve), here given mean values, could be varied with depth, nutrients, pigment composition, if information is available.

Conversely, the other improvement should be a simplification of the model in view of a generalised application to large scale and incorporation into a data assimilation scheme. For computational and practical reasons, a certain degradation in the quality of the mixed-layer description has to be accepted, and the necessary averaging (in time and space) of the input parameters for this segment will result in less accurate estimates of the mixed-layer depth and eddy diffusivities. The simplified version of the code, used when comparing the CO_2 evolution for the situations already studied by Taylor et al. (1991) is one possible approach. The sensitivity to a degraded representation of the mixed-layer characteristics has been tested, and unfortunately appears rather high. When using a degraded physical forcing, the introduction of the remotely-sensed SST certainly could preserve the simulation from excessive drifting. In summary, if satellite observations are definitely of unvaluable help in the biogeochemical problem of the pCO_2, if also numerical tools are in progress to make a meaningful use of these data, systematical field observations will be for a while absolutely necessary. The delineation of biogeochemical provinces tied to physical conditions, and a better knowledge of their own typical parameters, still require efforts as those planned in the frame of

JGOFS, before models become more efficient and realistic in their outputs.

6. Acknowledgements

We acknowledge support through the European Community contracts EPOC-CT90-0017 and ESCOBA EV5V-CT92-0124. The authors would like to express their appreciation to Annick Bricaud, Jean-François Minster, Jean-Michel André, and one anonymous reviewer for valuable criticism and suggestions. We are also grateful to Kaz Higuchi, Chi Shing Wong and Diana Ruiz-Pino for providing the data for station Papa.

REFERENCES

Antoine, D. and Morel, A. 1995. Modelling the seasonal course of the upper-ocean pCO_2. 1, Development of a one-dimensional model. *Tellus*, this issue.

Bacastow, R. and Maier-Reimer, E. 1990. Ocean-circulation model of the carbon cycle. *Climate Dyn.* **4**, 95–125.

Booth, B. C., Lewin, J. and Lorenzen, C. J. 1988. Spring and summer growth rates of subarctic Pacific phytoplankton assemblages determined from carbon uptake and cell volumes estimated using epifluorescence microscopy. *Mar. Biol.* **98**, 287–298.

Chan, Y. H. and Wong, C. S. 1990. Long-term changes in amplitudes of atmospheric CO_2 concentrations at Ocean Station P and Alert, Canada. *Tellus* **42B**, 330–341.

Deschamps, P. Y., Herman, M., Podaire, A., Leroy, M., Laporte, M. and Vermande, P. 1990. A spatial instrument for the observation of polarization and directionality of Earth reflectances: POLDER. In Remote sensing for the nineties, Proc. 10th IGARSS, 20–24 May 1990, Washington DC, IEEE catalog No. 90CH2825-8, IEEE, New-York, vol. III, 1769–1774.

Dugdale, R. C., Morel, A., Bricaud, A. and Wilkerson, F. P. 1989. Modeling new production in upwelling centers: a case study of modeling new production from remotely sensed temperature and color. *J. Geophys. Res.* **94**, 18119–18132.

Emerson, S. 1987. Seasonal oxygen cycles and biological new production in surface waters of the subarctic Pacific ocean. *J. Geophys. Res.* **92**, 6535–6544.

Emerson, S., Quay, P., Stump, C. D., Wilbur, C. and Knox, M. 1991. O_2, Ar, N_2 and ^{222}Rn in surface waters of the subarctic ocean: net biological O_2 production. *Global Biogeochem. Cycles* **5**, 49–69.

Eppley, R. W. and Peterson, B. J. 1979. Particulate organic matter flux and planktonic new production in the deep ocean. *Nature* **282**, 677–680.

Erickson, III D. J. 1989. Variations in the global air–sea transfer velocity field of CO_2. *Global Biogeochem. Cycles* **3**, 37–41.

Etcheto, J. and Merlivat, L. 1988. Satellite determination of the carbon dioxide exchange coefficient at the ocean-atmosphere interface: a first step. *J. Geophys. Res.* **93**, 15669–15678.

Etcheto, J., Boutin, J. and Merlivat, L. 1991. Seasonal variation of the CO_2 exchange coefficient over the global ocean using satellite wind speed measurements. *Tellus* **43B**, 247–255.

Frost, B. W. 1991. The role of grazing in nutrient-rich areas of the open ocean. *Limnol. Oceanogr.* **36**, 1616–1630.

Garçon, C., Thomas, F., Wong, C. S. and Minster, J. F. 1992. Gaining insight into the seasonal variability of CO_2 at ocean station P using an upper ocean model. *Deep-Sea Res.* **39**, 921–938.

Gaspar, P. 1988. Modeling the seasonal cycle of the upper ocean. *J. Phys. Oceanogr.* **18**, 161–180.

Gaspar, P., Gregoris, Y. and Lefevre, J. M. 1990. A simple eddy kinetic energy model for simulations of the oceanic vertical mixing: tests at station Papa and Long-Term Upper Ocean Study site. *J. Geophys. Res.* **95**, 16179–16193.

Hooker, S. B., Esaias, W. E., Feldman, G. C., Gregg, W. W. and McClain, C. R. 1992. *SeaWIFS Technical Report Series*, vol. 1. *An overview of SeaWIFS and Ocean Color.* NASA technical memorandum 104566.

Kamykowski, D. and Zentara, S. J. 1986. Predicting plant nutrient concentrations from temperature and sigma-*t* in the upper kilometer of the world ocean. *Deep-Sea Res.* **33**, 89–105.

Large, W. G., McWilliams, J. C. and Niiler, P. P. 1986. Upper ocean thermal response to strong autumnal forcing of the Northeast Pacific. *J. Phys. Oceanogr.* **16**, 1524–1550.

Levitus, S. 1982. *Climatological atlas of the world ocean.* NOAA prof pap. 13, US Govt. Print. Off., Washington, DC.

McAllister, C. D. 1969. Aspects of estimating zooplankton production from phytoplankton production. *J. Fish. Res. Bd. Can.* **26**, 199–220.

McAllister, C. D., Parsons, T. R. and Strickland, J. D. H. 1960. Primary productivity and fertility at station "P" in the North-east Pacific ocean. *J. Cons. Cons. Int. Explor. Mer.* **35**, 240–259.

Martin, P. J. 1985. Simulation of the mixed layer at OWS November and Papa with several models. *J. Geophys. Res.* **90**, 903–916.

Metzl, N., Beauverger, C., Brunet, C., Goyet, C. and Poisson, A. 1991. Surface water carbon dioxide in the

Southwest Indian sector of the Southern ocean: a highly variable CO_2 source/sink region in summer. *Mar. Chem.* **35**, 85–95.

Miller, C. B., Frost, B. W., Wheeler, P. A., Landry, M. R., Welschmeyer, N. and Powell, T. M. 1991. Ecological dynamics in the subarctic Pacific, a possibly iron-limited ecosystem. *Limnol. Oceanogr.* **36**, 1600–1615.

Morel, A. and Berthon, J. F. 1989. Surface pigments, algal biomass profiles, and potential production of the euphotic layer: relationships reinvestigated in view of remote-sensing applications. *Limnol. Oceanogr.* **34**, 1545–1562.

N.C.A.R. 1988. *Global distribution of total cloud cover and cloud type amount over the ocean.* NCAR technical notes. NCAR/TN-317 + STR.

Platt, T., Harisson, W. G., Lewis, M. R., Li, W. K. W., Sathyendranath, S., Smith, R. E. and Vezina, A. F. 1989. Biological production of the oceans: the case for a consensus. *Mar. Ecol. Prog. Ser.* **52**, 77–88.

Poisson, A., Metzl, N., Brunet, C., Schauer, B., Bres, B., Ruiz-Pino, D. and Louanchi, F. 1993. Variability of sources and sinks of CO_2 in the Western Indian and Southern Oceans during the year 1991. *J. Geophys. Res.* **98**, 22759–22778.

Sathyendranath, S., Platt, T., Horne, E. P. W., Harrison, W. G., Ulloa, O., Outerbridge, R. and Hoepffner, N. 1991. Estimation of new production in the ocean by compound remote sensing. *Nature* **353**, 129–133.

Takahashi, T., Chipman, D. and Volk, T. 1983. Geographical, seasonal, and secular variations of the partial pressure of CO_2 in surface waters of the north Atlantic ocean: the results of the north Atlantic TTO program. In: *Proceedings: Carbon dioxide research conference: carbon dioxide, science and consensus.* CONF-820970, US department of energy, Washington DC, II,123–II,145.

Tans, P. P., Fung, I. Y. and Takahashi, T. 1990. Observational constraints on the global atmospheric CO_2 budget. *Science* **247**, 1431–1438.

Taylor, A. H., Watson, A. J., Ainsworth, M., Robertson, J. E. and Turner, D. R. 1991. A modelling investigation of the role of phytoplankton in the balance of carbon at the surface of the North Atlantic. *Global Biogeochem. Cycles* **5**, 151–171.

Thomas, F., Perigaud, C., Merlivat, L. and Minster, J. F. 1988. World-scale monthly mapping of the CO_2 ocean-atmosphere gas-transfer coefficient. *Phil. Trans. R. Soc. Lond.* **A325**, 71–83.

Thomas, F., Minster, J. F., Gaspar, P. and Gregoris, Y. 1993. Comparing the behaviour of two ocean surface models in simulating dissolved O_2 concentration at OWSP. *Deep-Sea Res.* **40**, 395–408.

Tricot, C. 1985. *Estimation des flux de chaleurs en surface à la station météo-Océanographique Papa.* Sci. Rep. 1985/9. Inst. d'Astron. et de Géophys. G. Lemaître, Univ. Cath. de Louvain, Belgium.

Watson, A. J., Robinson, C., Robinson, J. E., Williams, P. J. Le B. and Fasham, M. J. R. 1991. Spatial variability in the sink for atmospheric carbon dioxide in the North Atlantic, *Nature* **350**, 50–53.

Wheeler, P. A. and Kokkinakis, S. A. 1990. Amonium recycling limits nitrate use in the oceanic subarctic Pacific. *Limnol. Oceanogr.* **35**, 1267–1278.

Wong, C. S. and Chan, Y. H. 1991. Temporal variations in the partial pressure and flux of CO_2 at ocean station P in the subarctic northeast Pacific ocean. *Tellus* **43B**, 206–223.

Yoder, J. A., McClain, C. R., Feldman, G. C. and Esaias, W. E. 1993. Annual cycles of phytoplankton chlorophyll concentrations in the global ocean: a satellite view. *Global Biogeochem. Cycles* **7**, 181–193.